Received: 3 June 2022 | Revised: 13 July 2022 | Accepted: 15 July 2022

DOI: 10.1002/ardp.202200295

FULL PAPER

ARCH PHARM DPhG
Archiv der Pharmazie

New antiproliferative agents derived from tricyclic 3,4-dihydrobenzo[4,5]imidazo[1,2-*a*][1,3,5]triazine scaffold: Synthesis and pharmacological effects

Marco Robello[1] | Silvia Salerno[2,3] | Elisabetta Barresi[2,3] | Paola Orlandi[4] | Francesca Vaglini[5] | Marta Banchi[4] | Francesca Simorini[2] | Emma Baglini[2] | Valeria Poggetti[2] | Sabrina Taliani[2,3] | Federico Da Settimo[2,3] | Guido Bocci[3,4]

[1]Synthetic Bioactive Molecules Section, LBC, NIDDK, NIH, Bethesda, Maryland, USA

[2]Department of Pharmacy, University of Pisa, Pisa, Italy

[3]Center for Instrument Sharing of the University of Pisa (CISUP), University of Pisa, Pisa, Italy

[4]Department of Clinical and Experimental Medicine, University of Pisa, Pisa, Italy

[5]Department of Translational Research and New Technologies in Medicine and Surgery, University of Pisa, Pisa, Italy

Correspondence
Sabrina Taliani, Department of Pharmacy, University of Pisa, via Bonanno 6, 56126 Pisa, Italy.
Email: sabrina.taliani@unipi.it

Funding information
University of Pisa, PRA Project, Grant/Award Number: PRA_2020_58

Abstract

A series of novel 3,4-dihydrobenzo[4,5]imidazo[1,2-*a*][1,3,5]triazine (BIT) derivatives were designed and synthesized. In vitro antiproliferative activity was detected toward two human colorectal adenocarcinoma cell lines (CaCo-2 and HT-29) and one human dermal microvascular endothelial cell line (HMVEC-d). The most active compounds, namely **2-4** and **8**, were further investigated to clarify the mechanism behind their biological activity. Through immunofluorescence assay, we identified the target of these molecules to be the microtubule cytoskeleton with subsequent formation of dense microtubule accumulation, particularly at the periphery of the cancer cells, as observed in paclitaxel-treated cells. Overall, these results highlight BIT derivatives as robust and feasible candidates deserving to be further developed in the search for novel potent antiproliferative microtubule-targeting agents.

KEYWORDS
[1,3,5]triazine, antiproliferation, antitumor agents, medicinal chemistry, small ring systems

1 | INTRODUCTION

In recent years, cancer death rates have continued to decline in both men and women due to improvements in treatments and prevention. On the other hand, the number of new diagnoses continuously rises, making cancer a growing public health problem with an estimated seven million new cases each year worldwide.[1,2]

Suitable prevention measures and high-quality screening for early diagnosis can help to contain the global burden, but these strategies must be accompanied by effective therapeutic treatments to increase patients' survival rates and improve their quality of life. Thus, a worldwide effort is underway in the medicinal chemistry community to find new anticancer drugs. The efficacy plateau achieved by conventional chemotherapeutic agents against most solid malignant tumors, the numerous side effects of the current drugs, as well as the increasing drug resistance of tumors, force the continuous search for new molecules with a safer effect profile.[3]

Usually, synthetic anticancer compounds have been structurally characterized by the presence of a heterocyclic core. A simple glance

at food and drug administration (FDA) databases reveals the structural significance of heterocycles in drug design and engineering of pharmaceuticals, making heterocycle-based compounds true cornerstones of medicinal chemistry thanks to their intrinsic versatility and unique physicochemical properties. Putting aside the already marketed drugs, there are numerous examples of such derivatives investigated for their promising activity against different malignancies, and anticancer research has been capitalizing on the tunable and dynamic core scaffold of these compounds.[4]

The incorporation of heterocyclic rings containing oxygen, nitrogen, or sulfur heteroatom(s) allows for modulating important pharmaceutical parameters, such as lipophilicity, polarity, and aqueous solubility in pursuance of obtaining lead compounds with improved biological and physicochemical features.[5]

Nitrogen-containing heterocycles represent the core structure of many drug candidates with a broad spectrum of pharmaceutical applications and therapeutic perspectives. Not surprisingly, in FDA databases nearly 60% of novel small-molecule drugs contain nitrogen-based heterocycles. In this context, five-membered heterocycles containing both an oxygen and a nitrogen atom, such as isoxazoles (also named 1,2-oxazoles), have gained particular relevance. Additionally, the isoxazole core attracts considerable attention in medicinal chemistry due to its straightforward synthetic access and ability to form multiple types of interactions with enzymes and receptors, conferring to this moiety the potential as a privileged motif for the development of compounds showing a plethora of different biological activities, including analgesic, antimicrobial, antiviral, anticonvulsant, antidepressant, antituberculosis, and immunosuppressant effects.[6] Of note, the isoxazole ring represents a common feature of numerous anticancer agents.[7,8] Among these, the class of diarylisoxazoles has been widely studied and has shown strong growth inhibitory activities against various human cancer cell lines[7,9–11]: 3,5-bis(3′-indolyl)isoxazoles **I** (Figure 1) exhibited in vitro cytotoxicity in the micromolar range[12] and 4-phenylisoxazoles **II** (Figure 1) displayed the inhibitory activity of bromodomain–histone interactions, eliciting antiproliferative and anti-inflammatory effects.[13] In addition, some compounds featuring structure **III** (Figure 1) showed potent growth inhibitory activities against a number of human cancer cell lines. The isoxazole ring was introduced as a mimic of the cis-alkenyl bridge of natural product combrestatin (CA-4), stabilizing the active cis orientation.[14]

For more than three decades, our research has been dedicated to the synthesis and biological evaluation of polyheterocyclic compounds as new antiproliferative agents.[15–20] Most of the reported compounds are characterized by tri- or tetra-cyclic systems bearing a pendant aryl group and/or a dialkylaminoalkyl side chain bounded to appropriate positions of the scaffold, targeting simultaneously multiple kinase pathways involved in angiogenesis and tumor growth, or exerting DNA intercalating activity and/or topoisomerase I/II (Topo I/II) poisoning effects, respectively. Examples from our in-house database of antiproliferative agents are represented by the tricyclic compounds of series **IV**,[16,18,20] **V**,[21,22], and **VI**[15] (Figure 1) that feature a heterotricyclic system decorated at different positions of the scaffold with a pendant phenyl ring variously functionalized with groups, such as OCH_3, Cl, and NO_2.

Aiming to search for new small molecules as antiproliferative agents and taking advantage of our long experience in the synthesis of heterocyclic compounds,[15–20,23–25] we investigated a small library of molecules based on the tricyclic 3,4-dihydrobenzo[4,5]imidazo[1,2-*a*][1,3,5]triazine (BIT, **1-9**, Figure 1) scaffold, in which a substituted phenyl ring was inserted at position 4, recalling the pendant aryl group characterizing our previously discovered antiproliferative compounds. The s-triazine nitrogen heterocycle was inserted in the tricyclic BIT core structure due to the well-known antiproliferative and antiautophagic activity exerted by a number of its derivatives.[26–30] Moreover, position 2 was functionalized with an amide group variously decorated with a phenyl-substituted isoxazole moiety, in virtue of the considerable attention received by this five-membered heterocycle as a promising framework for the discovery of novel drugs with a wide spectrum of biological activities.[7,8]

The newly synthesized derivatives **1-9** were then evaluated for their ability to exert antiproliferative activity on two human colon cancer cell lines and a human dermal microvascular endothelial cell line. For the most promising compounds, further assays were performed to investigate the mechanism underlying the antiproliferative effect.

2 | RESULTS AND DISCUSSION

2.1 | Chemistry

The synthesis of the target compounds **1-9** is reported in Scheme 1. We used the condensation of commercially available 2-guanidinobenzimidazole **10** with the appropriate benzaldehyde **11a-c** in refluxing ethanol, in the presence of piperidine, to obtain the triazine derivatives **12a-c**.

Then, the appropriate arylisoxazole carboxylic acid **13a-c** was dissolved in anhydrous dimethylformamide (DMF) and treated with N,N'-carbonyldiimidazole (CDI), under a nitrogen atmosphere. The reaction mixture was stirred at room temperature for 1 h, supplemented with the appropriate 4-aryl-3,4-dihydrobenzo[4,5]imidazo[1,2-*a*][1,3,5]triazin-2-amine **12a-c**, and left at room temperature for 18–24 h. The obtained precipitate was collected by vacuum filtration and recrystallized from DMF to obtain the target compounds **1-9**. In this study, no enantiomeric resolution was performed on the compounds and their biological properties were preliminarily evaluated on the racemic mixtures.

2.2 | Biology

The newly synthesized compounds **1-9** were evaluated for their ability to exert an antiproliferative activity by means of an inhibition growth assay on two human colorectal adenocarcinoma cell lines (CaCo-2 and HT-29) and one human dermal microvascular

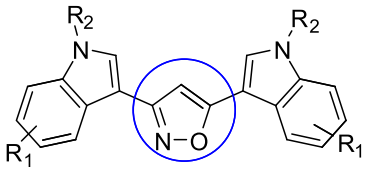

I

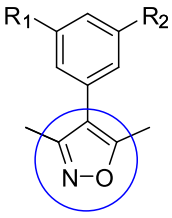

II

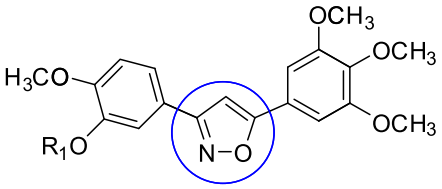

III

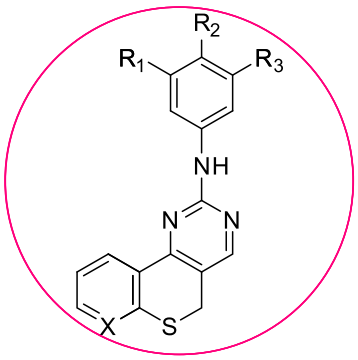

IV

R_1 = H,OCH_3; R_2 = OCH_3,Cl,NO_2
R_3 = H,OCH_3; X = CH,N

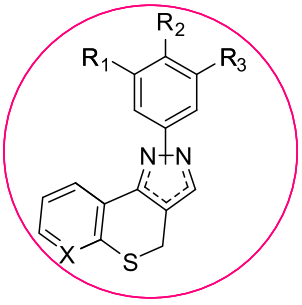

V

R_1, R_3 = H; R_2 = H,OCH_3,Cl,NO_2
X = CH,N

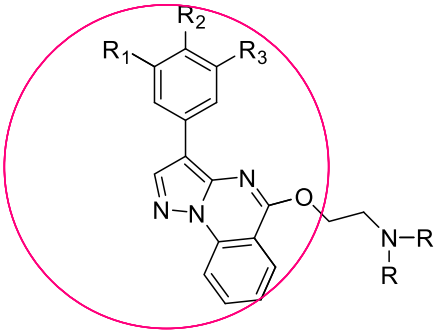

VI

R = CH_3,CH_2CH_3; R_1, R_3 = H
R_2 = OCH_3,Cl,NO_2

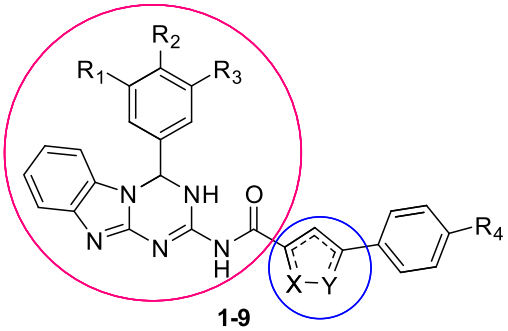

1-9

R_1 = H,OCH_3; R_2 = OCH_3,NO_2;
R_3 = H,OCH_3; R_4 = H,Cl; X,Y = N,O

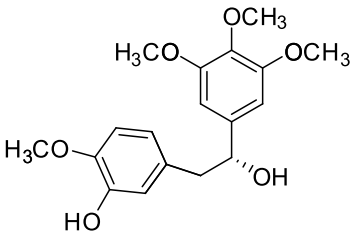

Combrestatin

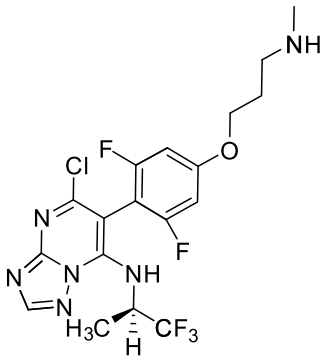

TTI-237

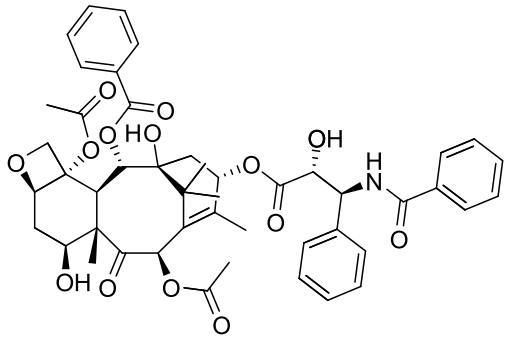

Paclitaxel

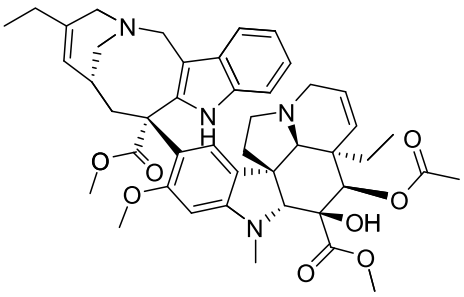

Vinorelbine

FIGURE 1 General structures of known diarylisoxazoles (I-III) and polyheterocyclic compounds (IV-VI) with growth inhibitory activities against various human cell lines. General structure of the newly developed 3,4-dihydrobenzo[4,5]imidazo [1,2-a][1,3,5]triazine derivatives (1-9). Structures of combrestatin, TTI-237, paclitaxel, and vinorelbine.

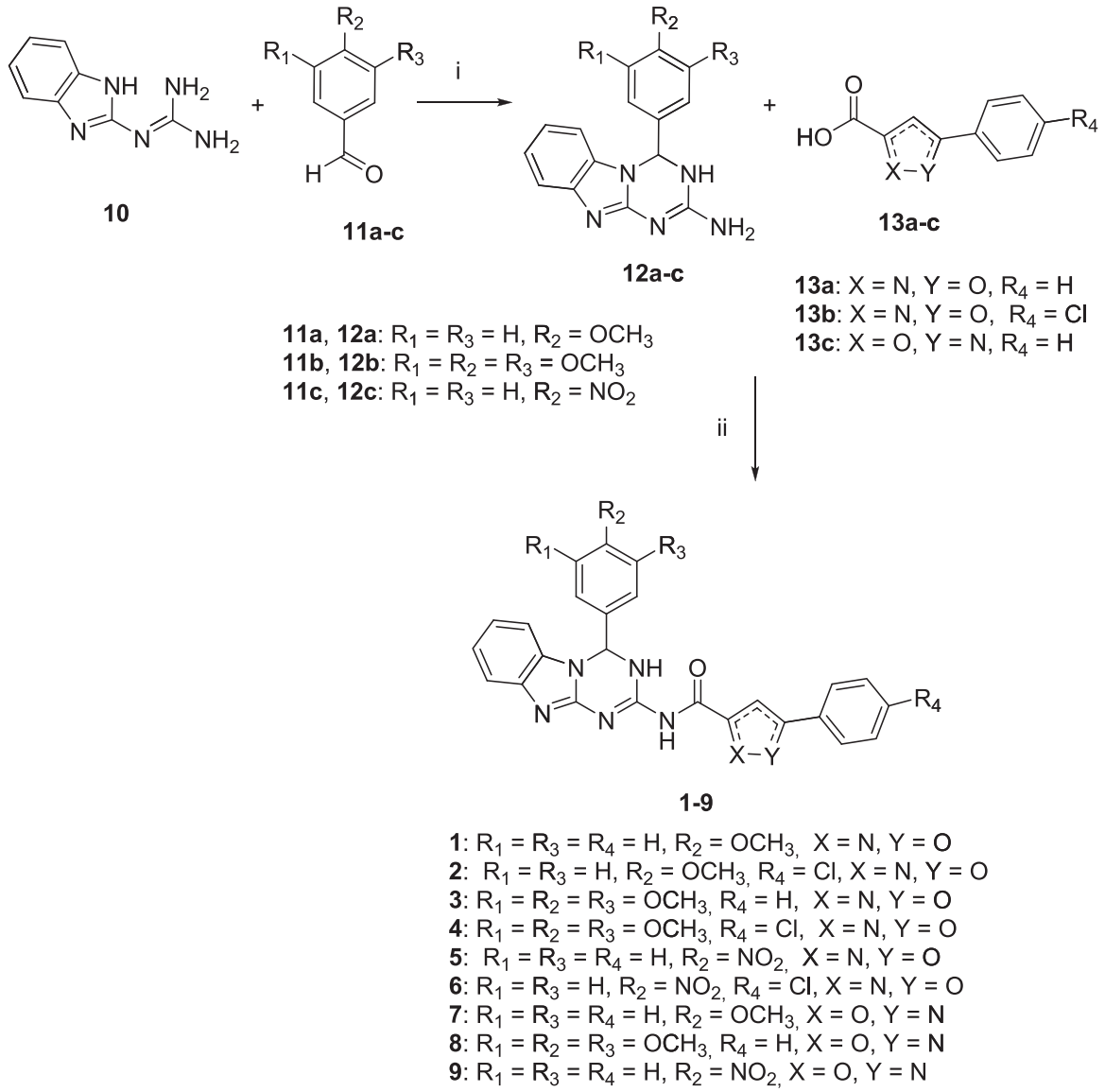

SCHEME 1 Synthesis of the new 3,4-dihydrobenzo[4,5]imidazo[1,2-*a*][1,3,5]triazino derivatives **1-9**

endothelial cell line (HMVEC-d). The antiproliferative parameters, expressed in terms of IC_{50} values obtained after 72 h of drug exposure, are listed in Table 1.

In general, all tested compounds **1-9** showed a concentration-dependent proliferation inhibition on all tested cancer (HT-29 and CaCo-2) and endothelial cells (HMVEC-d). Marked differences in potency were noted among the selected cell lines (Supporting Information: Figures S3-S11), with HMVEC-d resulting as the most sensitive one to all tested compounds (e.g., IC_{50} 4.45 μM) compared with CaCo-2 and HT-29 (e.g., IC_{50} values 19.36 and 15.24 μM, respectively), (Table 1).

In particular, among the 5-arylisoxazole-3-carboxamide subseries (compounds **1-6**), compounds **3** and **4** ($R_1 = R_2 = R_3 = OCH_3$, R_4 = H or and Cl, respectively) were the most interesting ones, inhibiting HMVEC-d cell proliferation with IC_{50} values of 5.18 and 4.45 μM, respectively. A lower, but still interesting, antiproliferative effect on HMVEC-d was also shown by compounds **2** ($R_1 = R_3$ = H, $R_2 = OCH_3$, R_4 = Cl), **5** ($R_1 = R_3$ = H, $R_2 = NO_2$, R_4 = H) and **6** ($R_1 = R_3$ = H, $R_2 = NO_2$, R_4 = Cl), with IC_{50} values of 10.86, 13.19, and 19.69 μM, respectively. Compound **1** represents the only exception to this general trend, showing limited antiproliferative activity on all three cell lines (IC_{50} values 26.68–>50 μM). The most active compounds in this subseries are **3** and **4**, bearing a 3′,4′,5′-trimethoxy decoration on the pendant phenyl ring at the 4 position of the BIT core, similar to that present in many anticancer drugs used in therapy.[31,32] The presence of a *p*-chlorine atom (R_4) on the 5-phenyl of the isoxazole linker seems to have different effects among series **3–6**. The effect is almost negligible when

TABLE 1 Growth Inhibition of Caco-2, HT-29, and HMVEC-d by compounds **1-9**

n	R_1	R_2	R_4	R_4	X	Y	IC_{50} (μM) Caco-2	IC_{50} (μM) HT-29	IC_{50} (μM) HMVEC-d
1	H	OCH_3	H	H	N	O	26.68 ± 0.38	33.82 ± 2.24	>50
2	H	OCH_3	H	Cl	N	O	19.36 ± 3.71	19.29 ± 2.62	10.86 ± 0.08
3	OCH_3	OCH_3	OCH_3	H	N	O	40.36 ± 0.25	>50	5.18 ± 0.97
4	OCH_3	OCH_3	OCH_3	Cl	N	O	32.02 ± 4.10	>50	4.45 ± 0.64
5	H	NO_2	H	H	N	O	>50	>50	13.19 ± 1.09
6	H	NO_2	H	Cl	N	O	22.25 ± 0.13	>50	19.69 ± 1.53
7	H	OCH_3	H	H	O	N	>50	>50	20.84 ± 1.47
8	OCH_3	OCH_3	OCH_3	H	O	N	>50	15.24 ± 1.29	13.39 ± 0.19
9	H	NO_2	H	H	O	N	>50	>50	>50

Note: The IC_{50} was calculated by nonlinear regression fit of the mean values of data obtained in triplicate experiments (at least nine wells for each concentration).

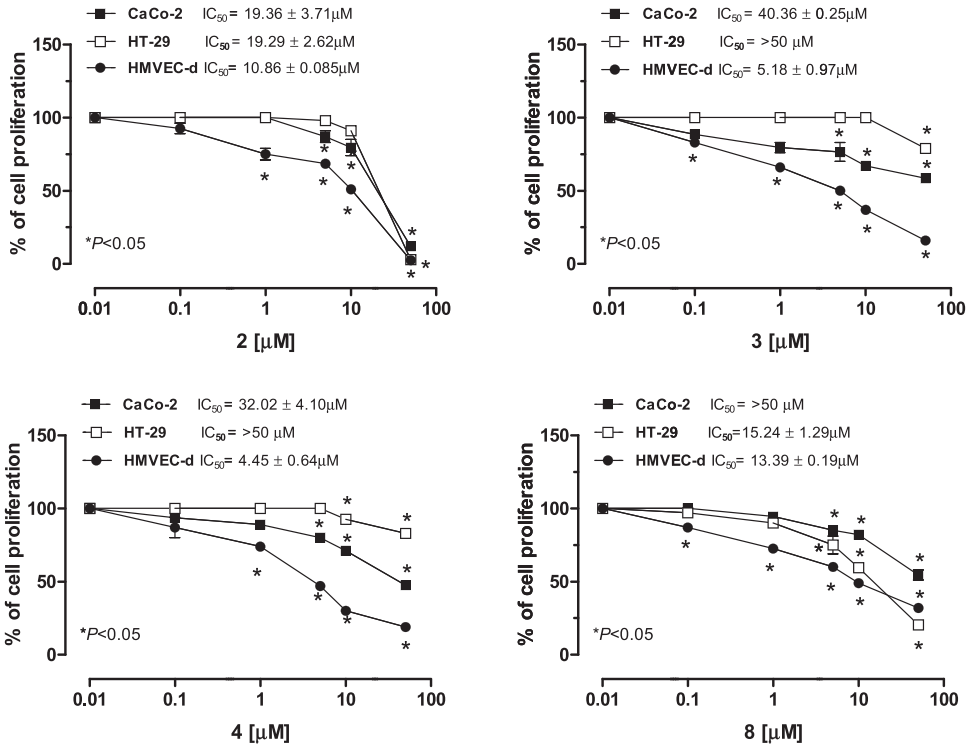

FIGURE 2 Antiproliferative activity of compounds **2**, **3**, **4**, and **8** in CaCo-2, HT-29, and human dermal microvascular endothelial cell line (HMVEC-d) cells

comparing compounds **3** and **4**, with the major difference on CaCo-2 cell line (40.36 vs. 32.02 μM, respectively). If we compare the nitro-substituted derivatives **5** and **6**, the introduction of chlorine seems to have divergent effects depending on the cell line under investigation: a slight improvement of activity on CaCo-2 cells (> 50 and 22.25 μM for **5** and **6**, respectively), but an opposite effect on HMVEC-d cells (13.19 and 19.69 μM for **5** and **6**, respectively). It should also be indicated that on the HT-29 cell line only mono-methoxy derivatives **1-2** showed inhibitory activity. In addition, a certain enhancement of antiproliferative activity can be envisaged between **1** (R_4=H) and **2** (R_4=Cl), with the chloro-substituted derivative showing higher potency than the unsubstituted one on all three cell lines, reaching a fivefold higher activity on HMVEC-d cell line.

In the 3-arylisoxazole-5-carboxamide subseries (compounds **7-9**), in which the phenyl ring was interchanged with the BIT moiety on the isoxazole ring with respect to the previous subseries **1-6**, the most active derivative showed to be **8** ($R_1 = R_2 = R_3 = OCH_3$, $R_4 = H$), which inhibited HMVEC-d and HT-29 cell proliferation with IC_{50} values of 13.39 and 15.24 μM, respectively, thus confirming the importance of the trimethoxy decoration ($R_1 = R_2 = R_3 = OCH_3$) on the phenyl ring at the 4-position of the BIT scaffold for the biological activity. Interestingly, the interchange of the two moieties on the isoxazole ring was detrimental to activity on CaCo-2 cells without differences among the different groups on the phenyl at the 4 position. It also had a negative effect on nitro-derivatives against the HMVEC-d cell line, as can be seen comparing **5** with **9** (19.69 vs. >50 μM, respectively).

In Figure 2, graphs for the antiproliferative activity of the most performing compounds **2**, **3**, **4**, and **8** in CaCo-2, HT-29, and HMVEC-d cells are reported.

To search for the molecular mechanism underlying the antiproliferative activity exhibited by the new compounds, we investigated the ability of the most active compounds **2-4**, and **8** to inhibit extracellular signal-regulated kinases 1/2 (ERK1/2) phosphorylation pathway, one of the main cellular signaling pathways involved in cell proliferation.

ERK1/2 are highly homologous serine/threonine kinases that form a key node in the transduction of growth factor signals, regulating a range of cellular functions including cell survival, differentiation, proliferation, adhesion, and migration. Thus, the ERK1/2 pathway is one of the most important components of cell survival signaling networks, and the evaluation of the ability of a new antiproliferative agent to inhibit ERK1/2 phosphorylation activity might be considered the first-line assay to investigate its putative cellular mechanism of action.[33]

Compounds **2-4** and **8** were tested for their ability to inhibit ERK1/2 phosphorylation in the HT-29 cell line. As shown in Figure 3, these compounds did not exert any inhibition of ERK1/2 phosphorylation at concentrations corresponding to their experimental IC_{50}s. After exposure to compounds **2-4** and **8**, the quantity of the phosphorylated (e.g., active) form of ERK1/2 in HT-29 was augmented even after 72 h, although not significantly.

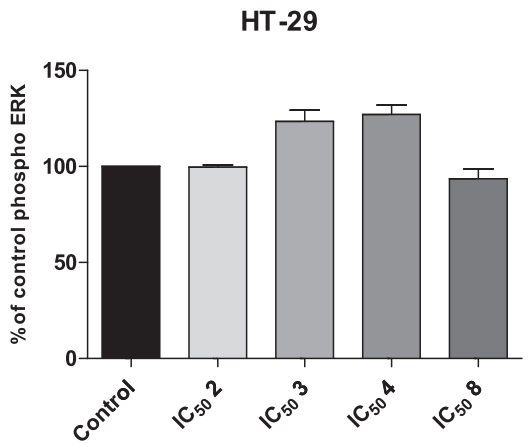

FIGURE 3 Extracellular signal-regulated kinases (ERK) phosphorylation by compounds **2-4** and **8** in the HT-29 cell line

As the results showed that the newly synthesized compounds did not interfere with tumor signaling pathways, we tried to identify another putative target responsible for the antiproliferative activity exerted by compounds **2-4** and **8**.

Our compounds display a diarylisoxazole structure and the most active ones bear a 3′,4′,5′-trimethoxy decoration on the pendant phenyl ring at the 4 position of the BIT core, resembling the structure of known microtubule-targeting agents (MTAs).[8]

MTAs are drugs largely used in the clinic (e.g., taxanes, epothilones, vinca alkaloids, etc.)[34] as anticancer agents, due to their ability to influence essential processes for tumor growth.[35] In growing cells, microtubules (MT) are necessary for the formation of the mitotic spindle, which is essential in the cell division process.[36] Spindle formation can occur thanks to MT dynamic equilibrium through polymerization and depolymerization cycles, which consist of noncovalent binding of tubulin dimers to form the MT and subsequent depolymerization to return tubulin dimers.[37]

MTAs can be divided into two categories: microtubule-destabilizing agents (MDAs), which promote MT depolymerization (e.g. colchicine, the combretastatins, the *Vinca* alkaloids, etc.),[38] and microtubule-stabilizing agents (MSAs), which stabilize the polymerized form of MTs (e.g. the epothilones, paclitaxel, discodermolide, laulimalide, eleutherobin, etc.).[39] At low concentrations, both MDAs and MSAs can arrest the mitotic cycle blocking MT dynamics without affecting MT mass.[40]

In this scenario, TTI-237 (Figure 1), a [1,2,4]triazolo[1,5-*a*]pyrimidine (TP)[41] emerged due to its unique features: it has been described as a cytotoxic agent with MT-stabilizing activity, but it also binds to vinblastine binding site on tubulin, which is typically targeted by MDAs. These particular properties could make TPs the prototype of new MT active compounds. In fact, the tricyclic 3,4-dihydrobenzo[4,5]imidazo[1,2-*a*][1,3,5]triazine scaffold of compounds **1-9** can be considered an enlargement of the bicyclic [1,2,4]triazolo[1,5-*a*]pyrimidine core present in the structure of TTI-237.

To investigate the putative cellular mechanism of action of our BIT derivatives **1-9**, we tested the most active compounds **2-4** and **8** for their ability to interfere with MT dynamic equilibrium by means of an immunofluorescence assay on the MT cytoskeleton of HT-29 cells.

HT-29 cells were incubated for 24 h with paclitaxel (Figure 1, MSA reference compound), vinorelbine (Figure 1, MDA reference compound), or compounds **2-4** and **8** at the concentration of 10 μM. The immunofluorescence images (Figure 4) clearly showed that the compounds target the MT cytoskeleton and induce the formation of dense, irregular MT accumulation, in particular at the periphery of the cancer cell (Figure 4). This is a structural feature similar to paclitaxel-treated cells (Figure 4), when compared with control cells. The cellular effects of compounds **2–4** and **8** were in contrast with those

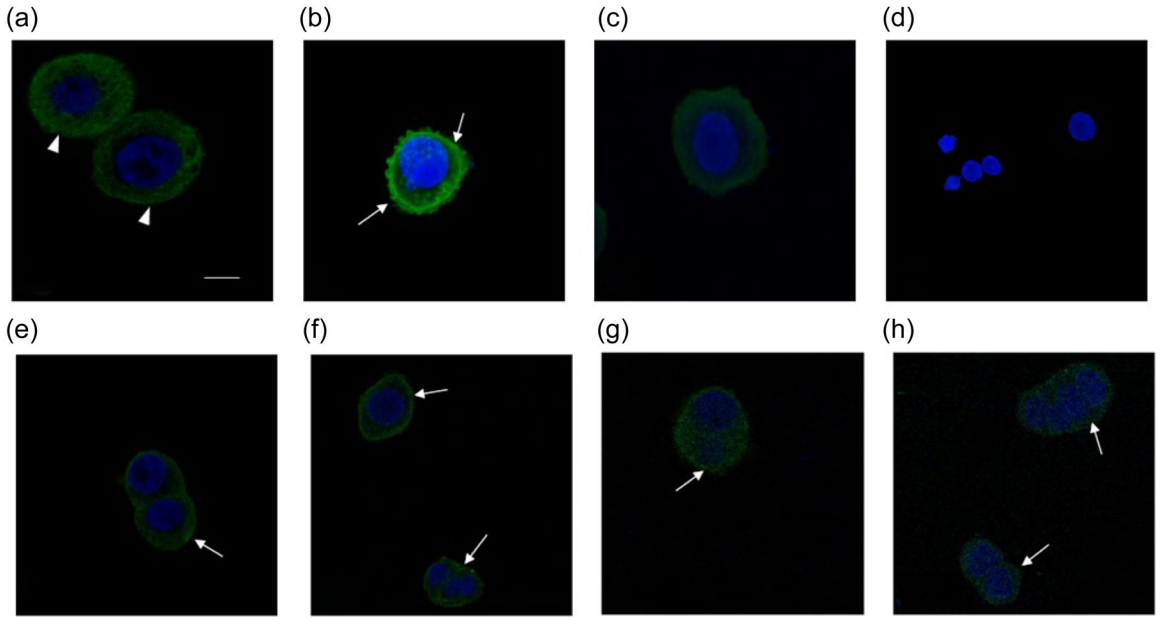

FIGURE 4 Representative images of HT29 cells immunostained for anti-A-tubulin (FITC, green) and DNA (DAPI blue). (a) Vehicle-treated cells, (b) paclitaxel 500 nM, (c) vinorelbine 100 pM, (d) no primary antibody (e), **2** 10 μM, (f) **3** 10 μM, (g) **4** 10 μM, and (h) **8** 10 μM. Arrowhead, normal microtubule structures; white arrows indicate irregular microtubule polymerization at the periphery of the cell cytoplasm. Scale bar: 50 μm.

observed with vinorelbine, which completely disaggregated the cytoplasmic MT network of HT-29 cells (Figure 4).

From these data, it seems reasonable to suppose that the antiproliferative activity exerted by our BIT compounds **2-4** and **8** is at least in part ascribable to their ability to stabilize the polymerized form of MTs, thus blocking MT dynamics, which in turn leads to the arrest of dividing cells in mitosis.

3 | CONCLUSION

We investigated a small library of heterocyclic derivatives which feature motifs characterizing the structures of many antiproliferative compounds discovered by us, along with the five-membered heterocycle isoxazole, which has been variously exploited for the discovery of novel drugs. Thus, the tricyclic 3,4-dihydrobenzo[4,5]imidazo[1,2-*a*][1,3,5]triazine (BIT) scaffold was decorated with a substituted phenyl ring at 4-position, and an amide group variously decorated with a phenyl-substituted isoxazole moiety at 2-position, to yield compounds **1-9**.

When evaluated for their ability to exert an antiproliferative activity on two human colorectal adenocarcinoma cell lines (CaCo-2 and HT-29) and one human dermal microvascular endothelial cell line (HMVEC-d), all compounds **1-9** showed a concentration-dependent proliferation inhibition against all the cell lines investigated, with the HMVEC-d being the most sensitive one.

The most active antiproliferative compounds were found to be **2-4** and **8**, and they were further investigated to clarify the mechanism underlying their biological activity. At first, the ability of compounds **2-4**, and **8** (Figure 3) to inhibit the ERK1/2 phosphorylation pathway was assessed in the HT-29 cell line. None of the tested compounds exerted inhibition of ERK1/2 phosphorylation at concentrations corresponding to their experimental IC_{50}s. Then, the structural similarity with some MTAs prompted us to test compounds **2-4** and **8** for their ability to interfere with MT dynamic equilibrium by means of an immunofluorescence assay on the MT cytoskeleton of HT-29 cells, comparing them with paclitaxel (MSA reference compound) and vinorelbine (MDA reference compound). Our results clearly showed that these compounds target the MT cytoskeleton and induce the formation of dense MT accumulation, in particular at the periphery of the cancer cell, similarly to paclitaxel-treated cells.

Taken together, these results were extremely encouraging as they identify BIT derivatives as valid candidates for further investigations in the search for novel potent antiproliferative MTAs.

4 | EXPERIMENTAL

4.1 | Chemistry

4.1.1 | General

^{1}H NMR spectra were obtained on a Bruker AVANCE 400 in hexadeuterated dimethylsulfoxide (DMSO-d_6). Chemical shifts (δ) are expressed in ppm and coupling constants (J) in Hertz. High-resolution ESI-MS spectra were performed on a Thermo LTQ Orbitrap XL mass spectrometer (Thermo Fisher Scientific). The spectra were recorded by infusion into the ESI source using MeOH as the solvent.

Evaporations were made in vacuo (rotating evaporator). Magnesium sulfate was used as the drying agent. Analytical TLC has been carried out on Merck 0.2-mm precoated silica gel aluminum sheets (60 F-254). Silica gel 60 (230–400 mesh) was used for column chromatography. The purity of the target compounds **1–9** was determined, using a Shimadzu LC-20AD SP liquid chromatograph equipped with a DDA detector at 254 nm [column C18 (250 mm, 4.6 mm, 5 µm, Shim-pack)]. The mobile phase, delivered at isocratic flow, consisted of methanol (95%) and water (5%) and a flow rate of 1.0 ml/min. All the compounds showed percent purity values ≥ 95%. Reagents, starting materials, and solvents were purchased from commercial suppliers and used as received. 4-(4-Methoxyphenyl)-3,4-dihydrobenzo[4,5]imidazo[1,2-*a*][1,3,5]triazin-2-amine **12a**, 4-(3,4,5-trimethoxyphenyl)-3,4-dihydrobenzo[4,5]imidazo[1,2-*a*][1,3,5]triazin-2-amine **12b** and 4-(4-nitrophenyl)-3,4-dihydrobenzo[4,5]imidazo[1,2-*a*][1,3,5]triazin-2-amine **12c** were obtained according to a previously described procedure.[42,43]

The InChI codes of the investigated compounds, together with some biological activity data, are provided in Supporting Information: Table S1.

4.1.2 | General procedure for the synthesis of 4-aryl-3,4-dihydrobenzo[4,5]imidazo[1,2-*a*][1,3,5]triazin-2-amines **12a-c**

A solution of 2-guanidinobenzimidazole **10** (1.752 g, 10.0 mmol), appropriate benzaldehyde **11a-c** (10.0 mmol), and 0.5 ml piperidine in ethanol (40 ml) was heated under reflux for 2.5 h. After cooling, the obtained suspension was filtered, and the crude collected product was recrystallized from ethanol.

*4-(4-Methoxyphenyl)-3,4-dihydrobenzo[4,5]imidazo[1,2-a][1,3,5]triazin-2-amine (**12a**)*[42]

Yield: 98%, m.p.: 246–247°C (m.p. lit.: 246–248°C)[42]; ^{1}H-NMR (400 MHz, DMSO-d_6) δ: 3.75 (s, 3H), 6.82 (d, 1H, J = 8.0 Hz), 6.82 (s, 1H), 6.99–7.03 (m, 3H), 7.13 (t, 1H, J = 7.8 Hz), 7.17 (s, 2H), 7.32 (d, 1H, J = 8.0 Hz), 7.42 (d, 2H, J = 8.8 Hz), 8.64 (s, 1H).

*4-(3,4,5-Trimethoxyphenyl)-3,4-dihydrobenzo[4,5]imidazo[1,2-a][1,3,5]triazin-2-amine (**12b**)*[43]

Yield: 75%, m.p.: 287–288°C (m.p. lit.: 288–290°C)[43]; ^{1}H-NMR (400 MHz, DMSO-d_6) δ: 3.64 (s, 3H), 3.71 (s, 6H), 6.36 (bs, 2H), 6.63 (s, 1H), 6.73 (s, 2H), 6.80 (s, 1H), 6.78–6.84 (m, 1H), 6.94 (t, 1H, J = 7.0 Hz), 7.24 (d, 1H, J = 8.0 Hz), 7.93 (s, 1H).

*4-(4-Nitrophenyl)-3,4-dihydrobenzo[4,5]imidazo[1,2-a][1,3,5]triazin-2-amine (**12c**)*[43]

Yield: 55%, m.p.: 225–226°C (m.p. lit.: 224–226°C)[43]; ^{1}H-NMR (400 MHz, DMSO-d_6) δ: 6.52 (bs, 2H), 6.80–6.88 (m, 2H), 6.94–6.96 (m, 2H), 7.26 (d, 1H, J = 7.6 Hz), 7.58 (d, 2H, J = 8.8 Hz), 8.16 (s, 1H), 8.27 (d, 2H, J = 8.8 Hz).

4.1.3 | General procedure for the synthesis of *N*-(4-aryl-3,4-dihydrobenzo[4,5]imidazo[1,2-*a*][1,3,5]triazin-2-yl)-5-arylisoxazole-3-carboxamides **1-6**

A mixture containing 0.45 mmol of the opportune 5-arylisoxazole-3-carboxylic acid **13a,b** and 146 mg (0.90 mmol) of CDI in 5.0 ml of anhydrous DMF, was stirred at room temperature for 1 h, under nitrogen atmosphere. Then, the appropriate 4-aryl-3,4-dihydrobenzo[4,5]imidazo[1,2-*a*][1,3,5]triazin-2-amine **12a-c** (0.45 mmol) was added and the mixture was left at room temperature for 18–24 h (TLC analysis DCM/MeOH 9:1). The obtained precipitate was collected by vacuum filtration and recrystallized from DMF to obtain compounds **1-6**.

*N-[4-(4-Methoxyphenyl)-3,4-dihydrobenzo[4,5]imidazo[1,2-a][1,3,5]triazin-2-yl]-5-phenylisoxazole-3-carboxamide (**1**)*

Yield: 25%, m.p.: 210–211°C; ^{1}H-NMR (400 MHz, DMSO-d_6) δ: 3.75 (s, 3H), 6.97–7.03 (m, 4H), 7.06 (s, 1H), 7.11 (t, 1H, J = 8.2 Hz), 7.40–7.46 (m, 4H), 7.56–7.60 (m, 3H), 7.94 (dd, 2H, J_{min} = 2.0 Hz, J_{max} = 8.2 Hz); ^{13}C-NMR (100 MHz, DMSO-d_6) δ: 55.69, 66.70, 100.78, 110.21, 114.88, 121.83, 122.91, 126.21, 126.81, 128.48, 129.84, 131.32, 160.59; HRMS (ESI) *m/z* Calcd for $C_{26}H_{21}N_6O_3^+$: 465.16715; Found: 465.16728 $[M+H]^+$.

*5-(4-Chlorophenyl)-N-[4-(4-methoxyphenyl)-3,4-dihydrobenzo[4,5]imidazo[1,2-a][1,3,5]triazin-2-yl]isoxazole-3-carboxamide (**2**)*

Yield: 47%, m.p.: 243–244°C; ^{1}H-NMR (400 MHz, DMSO-d_6) δ: 3.74 (s, 3H), 6.97–7.12 (m, 6H), 7.40–7.45 (m, 4H), 7.65 (d, 2H, J = 8.0 Hz), 7.97 (d, 2H, J = 8.4 Hz); ^{13}C-NMR (100 MHz, DMSO-d_6) δ: 55.70, 66.62, 101.39, 110.21, 114.90, 121.63, 122.69, 125.58, 128.04, 128.48, 129.95, 135.93, 160.61; HRMS (ESI) *m/z* Calcd for $C_{26}H_{20}ClN_6O_3^+$: 499.12854; Found: 499.12872 $[M+H]^+$.

*5-Phenyl-N-[4-(3,4,5-trimethoxyphenyl)-3,4-dihydrobenzo[4,5]imidazo[1,2-a][1,3,5]triazin-2-yl]isoxazole-3-carboxamide (**3**)*

Yield: 20%, m.p.: 204–205°C; ^{1}H-NMR (400 MHz, DMSO-d_6) δ: 3.65 (s, 3H), 3.73 (s, 6H), 6.83 (s, 2H), 7.01–7.04 (m, 3H), 7.11–7.14 (m, 1H), 7.45–7.47 (m, 2H), 7.58–7.60 (m, 3H), 7.93–7.95 (m, 2H); ^{13}C-NMR (100 MHz, DMSO-d_6) δ: 56.50, 60.50, 104.53, 110.25, 126.22, 126.84, 129.84, 131.19, 138.84, 153.73; HRMS (ESI) *m/z* Calcd for $C_{28}H_{25}N_6O_5^+$: 525.18864; Found: 525.18903 $[M+H]^+$.

*5-(4-Chlorophenyl)-N-[4-(3,4,5-trimethoxyphenyl)-3,4-dihydrobenzo[4,5]imidazo[1,2-a][1,3,5]triazin-2-yl]isoxazole-3-carboxamide (**4**)*

Yield: 37%, m.p.: 242–243°C; ^{1}H-NMR (400 MHz, DMSO-d_6) δ: 3.65 (s, 3H), 3.72 (s, 6H), 6.82 (s, 2H), 7.00–7.03 (m, 3H), 7.11–7.13 (m, 1H), 7.44–7.46 (m, 2H), 7.64 (d, 2H, J = 8.4 Hz), 7.97 (d, 2H, J = 8.4 Hz); ^{13}C-NMR (100 MHz, DMSO-d_6) δ: 56.52, 60.51, 101.36, 104.65, 107.39, 122.06, 128.07, 129.97, 136.12, 138.43, 153.74; HRMS (ESI) *m/z* Calcd for $C_{28}H_{24}ClN_6O_5^+$: 559.14912; Found: 559.14917 $[M+H]^+$.

N-*[4-(4-Nitrophenyl)-3,4-dihydrobenzo[4,5]imidazo[1,2-a][1,3,5]triazin-2-yl]-5-phenylisoxazole-3-carboxamide (**5**)*

Yield: 25%, m.p.: 206–207°C; ^{1}H-NMR (400 MHz, DMSO-d_6) δ: 7.02 (t, 1H, J = 7.6 Hz), 7.11–7.14 (m, 2H), 7.29 (s, 1H), 7.45–7.47 (m, 2H), 7.57–7.60 (m, 3H), 7.73 (d, 2H, J = 8.4 Hz), 7.92–7.95 (m, 2H), 8.28 (d, 2H, J = 8.4 Hz); ^{13}C-NMR (100 MHz, DMSO-d_6) δ: 65.99, 100.74, 109.99, 121.76, 122.90, 124.77, 125.56, 126.20, 126.75, 128.27, 129.84, 131.37, 146.29, 148.53, 170.89; HRMS (ESI) m/z Calcd for $C_{25}H_{18}N_7O_4^+$: 480.14203; Found: 480.14186 $[M+H]^+$.

*5-(4-Chlorophenyl)-*N*-[4-(4-nitrophenyl)-3,4-dihydrobenzo[4,5]imidazo[1,2-a][1,3,5]triazin-2-yl]isoxazole-3-carboxamide (**6**)*

Yield: 20%, m.p.: 221–222°C; ^{1}H-NMR (400 MHz, DMSO-d_6) δ: 7.00–7.04 (m, 1H), 7.10–7.14 (m, 2H), 7.29 (s, 1H), 7.45–7.47 (m, 2H), 7.65 (d, 2H, J = 8.0 Hz), 7.73 (d, 2H, J = 8.0 Hz), 7.96 (d, 2H, J = 8.0 Hz), 8.27 (d, 2H, J = 8.0 Hz); ^{13}C-NMR (100 MHz, DMSO-d_6) δ: 60.41, 101.34, 109.89, 121.48, 124.81, 125.56, 128.05, 128.43, 129.95, 148.55, 169.47; HRMS (ESI) m/z Calcd for $C_{25}H_{17}ClN_7O_4^+$: 514.10305; Found: 514.10327 $[M+H]^+$.

4.1.4 | General procedure for the synthesis of *N*-(4-aryl-3,4-dihydrobenzo[4,5]imidazo[1,2-*a*][1,3,5]triazin-2-yl)-3-arylisoxazole-5-carboxamides **7-9**

A mixture containing 100 mg (0.53 mmol) of 3-phenylisoxazole-5-carboxylic acid **13c** and 173 mg (1.06 mmol) of CDI in 5.0 ml of anhydrous DMF, was stirred at room temperature for 1 h, under nitrogen atmosphere. The appropriate 4-aryl-3,4-dihydrobenzo[4,5]imidazo[1,2-*a*][1,3,5]triazin-2-amine **12a-c** (0.53 mmol) was added and the reaction mixture was left at room temperature for 18–24 h (TLC analysis DCM/MeOH 9:1). The obtained precipitated was collected by vacuum filtration and washed with water to obtain compounds **7-9**.

N-*[4-(4-Methoxyphenyl)-3,4-dihydrobenzo[4,5]imidazo[1,2-a][1,3,5]triazin-2-yl]-3-phenylisoxazole-5-carboxamide (**7**)*

Yield: 46%, m.p.: 247–248°C; ^{1}H-NMR (400 MHz, DMSO-d_6) δ: 3.75 (s, 3H), 6.97–7.05 (m, 5H), 7.14 (t, 1H, J = 7.5 Hz), 7.42–7.47 (m, 3H), 7.54–7.56 (m, 3H), 7.62 (s, 1H), 7.92–7.94 (m, 2H); ^{13}C-NMR (100 MHz, DMSO-d_6) δ: 55.71, 66.62, 110.47, 114.93, 127.07, 127.78, 128.57, 129.70, 131.19, 152.66, 159.89, 160.66, 163.02; HRMS (ESI) m/z Calcd for $C_{26}H_{21}N_6O_3^+$: 465.16751; Found: 465.16739 $[M+H]^+$.

N-*[4-(3,4,5-Trimethoxyphenyl)-3,4-dihydrobenzo[4,5]imidazo[1,2-a][1,3,5]triazin-2-yl]-3-phenylisoxazole-5-carboxamide (**8**)*

Yield: 51%, m.p.: 237–238°C; ^{1}H-NMR (400 MHz, DMSO-d_6) δ: 3.66 (s, 3H), 3.73 (s, 6H), 6.84 (s, 2H), 7.01–7.07 (m, 3H), 7.13–7.17 (m, 1H), 7.47 (d, 1H, J = 7.6 Hz), 7.54–7.55 (m, 3H), 7.63 (s, 1H), 7.93–7.94 (m, 2H); ^{13}C-NMR (100 MHz, DMSO-d_6) δ: 56.53, 60.50, 67.33, 104.67, 105.75, 110.52, 116.89, 121.98, 122.90, 127.16, 128.51, 129.69, 131.00, 131.14, 134.32, 138.96, 153.78, 162.93; HRMS (ESI) m/z Calcd for $C_{28}H_{25}N_6O_5^+$: 525.18864; Found: 525.18838 $[M+H]^+$.

N-*[4-(4-Nitrophenyl)-3,4-dihydrobenzo[4,5]imidazo[1,2-a][1,3,5]triazin-2-yl]-3-phenylisoxazole-5-carboxamide (**9**)*

Yield: 30%, m.p.: 220–221°C; ^{1}H-NMR (400 MHz, DMSO-d_6) δ: 7.08–-7.12 (m, 1H), 7.19–7.22 (m, 2H), 7.34 (s, 1H), 7.50 (d, 1H, J = 8.0 Hz), 7.55–7.57 (m, 3H), 7.80 (d, 2H, J = 8.8 Hz), 7.91–7.94 (m, 2H), 8.29 (d, 2H, J = 8.8 Hz); ^{13}C-NMR (100 MHz, DMSO-d_6) δ: 65.84, 103.67, 110.47, 122.69, 127.05, 128.06, 128.28, 129.76, 131.21, 133.20, 137.78, 145.43, 148.51, 163.25; HRMS (ESI) m/z Calcd for $C_{25}H_{17}N_7O_4$: 480.14148; Found: 480.14130 $[M+H]^+$.

4.2 | Biological assays

4.2.1 | Materials, drugs, and cells lines

Recombinant human basic fibroblast growth factor (bFGF) and recombinant human epidermal growth factor (rhEGF) were from PeproTechEC Ltd. Dulbecco's Modified Eagle Medium (DMEM), MCDB131, Eagle's Minimum Essential Medium (EMEM), fetal bovine serum (FBS), L-glutamine, and antibiotics were from Gibco (ThermoFisher Scientific). Type A gelatin from porcine skin, supplements, and all other chemicals not listed in this section were from Sigma Chemical Co. Plastics for cell culture were supplied by Costar.

The human colon tumor cell lines HT-29 and CaCo-2 were obtained from the American Type Culture Collection and maintained in 10% FBS DMEM and EMEM media, respectively, supplemented with antibiotics and L-glutamine 2 mM. Human dermal microvascular endothelial cells (HMVEC-d; Clonetics) were maintained in an MCDB131 culture medium supplemented with antibiotics, 15% heat-inactivated FBS, L-glutamine (2 mM), heparin (10 IU/ml), rhEGF (10 ng/ml), and rhbFGF (5 ng/ml). Cell lines were routinely grown in tissue culture flasks and kept in a humidified atmosphere of 5% CO_2 at 37°C.

In vitro studies were performed using drugs diluted from a 10 mM stock solution (in 100% dimethylsulfoxide). In the in vitro experiments, negative controls had the same concentration of dimethylsulfoxide in the media as did cells that were treated with the highest concentration of **1-9**. Vinorelbine and paclitaxel were used as positive controls because of their known antiproliferative effect on endothelial cells.[44,45] Both drugs showed a strong antiproliferative activity on HMVEC-d cells after 72 h of treatment reaching an IC_{50} of 0.6 nM for paclitaxel and 0.2 nM for vinorelbine.

4.2.2 | In vitro studies

Cell proliferation assay

HT-29, CaCo-2, and HMVEC-d cells were plated in 24-well plates and allowed to attach overnight. Cells were treated with compounds **1-9** (0.01–50 μM) or with their vehicles for 72 h. At the end of the treatment, cells were harvested with trypsin/EDTA and viable cells were quantified by using the automatic cell counter ADAM MC Digital B (Digital Bio, NanoEnTek Inc. USA & Europe). The concentration of drug that reduced cell proliferation by 50% (IC_{50})

versus controls was calculated by nonlinear regression fit of the mean values of data obtained in triplicate experiments (at least 9 wells for each concentration).

ERK1/2 (pTpY185/187) ELISA assay

To detect the phosphorylation of ERK1/2 in HT-29 cancer cells after a 72 h drug treatment, cells were exposed to **1-9** at concentrations corresponding to the experimental IC_{50} or with a vehicle alone for 72 h. To measure phosphoERK1/2 (pERK1/2), at the end of the experiment, the cells were harvested and immediately frozen with liquid nitrogen. Cells were lysed as per the manufacturer's instructions. Each sample was then assayed for human ERK1/2 phosphorylation by the PhosphoDetect ERK1/2 (pThr185/pTyr187) ELISA Kit (Calbiochem), and the values normalized by total protein, as previously published.[46] The optical density was determined using the Multiskan Spectrum microplate reader set to 450 nm. The results were expressed as a percentage of pERK1/2 of controls. All experiments were repeated, independently, six times with at least nine samples for each concentration.

Immunofluorescence

HT29 cells were plated at a density of 8000 cells/well onto 12-mm round coverslips. The day after, the cells were treated with different compounds: vinorelbine 100 pM, paclitaxel 500 nM, **2** 10 μM, **3** 10 μM, **4** 10 μM, **8** 10 μM, and drugs vehicle. The previously described experimental procedure was followed with minor changes.[47] After 24 h, the cells were fixed with 4% para-formaldehyde for 1 h at room temperature and washed three times with PBS, then the cells were permeabilized with PBS-Triton X-100 0.2% solution. Nonspecific sites were blocked using a solution containing 1.5% of normal goat serum and later the cells were incubated overnight at 4°C with 1:400 of monoclonal antibody anti-A-tubulin (clone DM 1 A, Sigma Aldrich). The coverslips were washed three times with PBS overlaid with a secondary FITC goat-antimouse antibody (diluted 1:250 in PBS) and incubated for 90 min at room temperature in the dark. After three washes with PBS, DNA staining was performed using DAPI/antifade solution (Merck, Millipore S.A.S.). The samples were observed with a confocal laser scanning microscope at ×63 magnification (TC SSP8 Leica Microsystems) using 488-nm and 605-nm excitation wavelength lasers. Controls consisted of cells incubated without the primary antibody.

Statistical analysis of data

The analysis by analysis of variance (ANOVA), followed by the Student-Newman–Keuls test, was used to assess the statistical differences of data in vitro. *p*-values lower than 0.05 were considered significant. Statistical analyses were performed using the GraphPad Prism software package version 5.0 (GraphPad Software Inc.).

ACKNOWLEDGMENTS

The authors thank Dr. Anna Fioravanti for her technical assistance. This study was supported by the University of Pisa (PRA Project, PRA_2020_58). Open Access Funding provided by Universita degli Studi di Pisa within the CRUI-CARE Agreement. We would like to thank Alicia Lillich, NIH Library Editing Service, for reviewing the manuscript.

CONFLICTS OF INTEREST

The authors declare no conflicts of interest.

ORCID

Marco Robello https://orcid.org/0000-0002-5835-7796
Silvia Salerno https://orcid.org/0000-0002-6072-4698
Elisabetta Barresi https://orcid.org/0000-0002-9814-7195
Francesca Simorini https://orcid.org/0000-0002-6745-6489
Emma Baglini https://orcid.org/0000-0002-8378-4052
Valeria Poggetti https://orcid.org/0000-0003-1284-4991
Sabrina Taliani https://orcid.org/0000-0001-8675-939X
Federico Da Settimo https://orcid.org/0000-0002-7897-7917
Guido Bocci https://orcid.org/0000-0001-7120-9141

REFERENCES

[1] H. Sung, J. Ferlay, R. L. Siegel, M. Laversanne, I. Soerjomataram, A. Jemal, F. Bray, *CA Cancer J. Clin.* **2021**, *71*, 209.
[2] K. D. Miller, L. Nogueira, A. B. Mariotto, J. H. Rowland, K. R. Yabroff, C. M. Alfano, A. Jemal, J. L. Kramer, R. L. Siegel, *CA Cancer J. Clin.* **2019**, *69*, 363.
[3] F. Meric-Bernstam, G. B. Mills, *Nat. Rev. Clin. Oncol.* **2012**, *9*, 542.
[4] P. Martins, J. Jesus, S. Santos, L. R. Raposo, C. Roma-Rodrigues, P. V. Baptista, A. R. Fernandes, *Molecules* **2015**, *20*, 16852.
[5] G. Li Petri, S. Cascioferro, B. El Hassouni, D. Carbone, B. Parrino, G. Cirrincione, G. J. Peters, P. Diana, E. Giovannetti, *Anticancer Res.* **2019**, *39*, 3615.
[6] V. Spanò, R. Rocca, M. Barreca, D. Giallombardo, A. Montalbano, A. Carbone, M. V. Raimondi, E. Gaudio, R. Bortolozzi, R. Bai, P. Tassone, S. Alcaro, E. Hamel, G. Viola, F. Bertoni, P. Barraja, *J. Med. Chem.* **2020**, *63*, 12023.
[7] M. A. Chiacchio, G. Lanza, U. Chiacchio, S. V. Giofrè, R. Romeo, D. Iannazzo, L. Legnani, *Curr. Med. Chem.* **2018**, *26*, 7337.
[8] M. Barreca, V. Spanò, M. V. Raimondi, C. Tarantelli, F. Spriano, F. Bertoni, P. Barraja, A. Montalbano, *Eur. J. Med. Chem. Reports* **2021**, *1*, 100004.
[9] A. Y. Shaw, M. C. Henderson, G. Flynn, B. Samulitis, H. Han, S. P. Stratton, H.-H.H.S. Chow, L. H. Hurley, R. T. Dorr, *J. Pharmacol. Exp. Ther.* **2009**, *331*, 636.
[10] P. Barraja, L. Caracausi, P. Diana, V. Spanò, A. Montalbano, A. Carbone, B. Parrino, G. Cirrincione, *ChemMedChem* **2012**, *7*, 1901.
[11] P. A. Brough, W. Aherne, X. Barril, J. Borgognoni, K. Boxall, J. E. Cansfield, K. M. J. Cheung, I. Collins, N. G. M. Davies, M. J. Drysdale, B. Dymock, S. A. Eccles, H. Finch, A. Fink, A. Hayes, R. Howes, R. E. Hubbard, K. James, A. M. Jordan, A. Lockie, V. Martins, A. Massey, T. P. Matthews, E. McDonald, C. J. Northfield, L. H. Pearl, C. Prodromou, S. Ray, F. I. Raynaud, S. D. Roughley, S. Y. Sharp, A. Surgenor, D. L. Walmsley, P. Webb, M. Wood, P. Workman, L. Wright, *J. Med. Chem.* **2008**, *51*, 196.
[12] P. Diana, A. Carbone, P. Barraja, G. Kelter, H. H. Fiebig, G. Cirrincione, *Bioorg. Med. Chem.* **2010**, *18*, 4524.
[13] D. S. Hewings, M. Wang, M. Philpott, O. Fedorov, S. Uttarkar, P. Filippakopoulos, S. Picaud, C. Vuppusetty, B. Marsden, S. Knapp, S. J. Conway, T. D. Heightman, *J. Med. Chem.* **2011**, *54*, 6761.
[14] J. Kaffy, R. Pontikis, D. Carrez, A. Croisy, C. Monneret, J. C. Florent, *Bioorg. Med. Chem.* **2006**, *14*, 4067.
[15] S. Taliani, I. Pugliesi, E. Barresi, S. Salerno, C. Marchand, K. Agama, F. Simorini, C. La Motta, A. M. Marini, F. S. Di Leva, L. Marinelli,

S. Cosconati, E. Novellino, Y. Pommier, R. Di Santo, F. Da Settimo, *J. Med. Chem.* **2013**, *56*, 7458.
[16] S. Salerno, A. M. Marini, G. Fornaciari, F. Simorini, C. La Motta, S. Taliani, S. Sartini, F. Da Settimo, A. N. Garciá-Argaéz, O. Gia, S. Cosconati, E. Novellino, P. D'Ocon, A. Fioravanti, P. Orlandi, G. Bocci, L. Dalla Via, *Eur. J. Med. Chem.* **2015**, *103*, 29.
[17] S. Salerno, V. La Pietra, M. Hyeraci, S. Taliani, M. Robello, E. Barresi, C. Milite, F. Simorini, A. N. García-Argáez, L. Marinelli, E. Novellino, F. Da Settimo, A. M. Marini, L. Dalla Via, *Eur. J. Med. Chem.* **2019**, *165*, 46.
[18] S. Salerno, A. N. García-Argáez, E. Barresi, S. Taliani, F. Simorini, C. La Motta, G. Amendola, S. Tomassi, S. Cosconati, E. Novellino, F. Da Settimo, A. M. Marini, L. D. Via, *Eur. J. Med. Chem.* **2018**, *150*, 446.
[19] L. Dalla Via, S. M. Magno, O. Gia, A. M. Marini, F. Da Settimo, S. Salerno, C. La Motta, F. Simorini, S. Taliani, A. Lavecchia, C. Di Giovanni, G. Brancato, V. Barone, E. Novellino, *J. Med. Chem.* **2009**, *52*, 5429.
[20] S. Salerno, E. Barresi, A. N. García-Argáez, S. Taliani, F. Simorini, G. Amendola, S. Tomassi, S. Cosconati, E. Novellino, F. Da Settimo, A. M. Marini, L. Dalla Via, *ACS Med. Chem. Lett.* **2019**, *10*, 457.
[21] G. Primofiore, A. M. Marini, F. Da Settimo, S. Salerno, D. Bertini, L. D. Via, S. M. Magno, *J. Heterocycl. Chem.* **2003**, *40*, 783.
[22] L. Dalla Via, A. M. Marini, S. Salerno, C. La Motta, M. Condello, G. Arancia, E. Agostinelli, A. Toninello, *Bioorg. Med. Chem.* **2009**, *17*, 326.
[23] S. Taliani, I. Pugliesi, E. Barresi, F. Simorini, S. Salerno, C. La Motta, A. M. Marini, B. Cosimelli, S. Cosconati, S. Di Maro, L. Marinelli, S. Daniele, M. L. Trincavelli, G. Greco, E. Novellino, C. Martini, F. Da Settimo, *J. Med. Chem.* **2012**, *55*, 1490.
[24] A. M. Marini, A. Maresca, M. Aggarwal, E. Orlandini, S. Nencetti, F. Da Settimo, S. Salerno, F. Simorini, C. La Motta, S. Taliani, E. Nuti, A. Scozzafava, R. McKenna, A. Rossello, C. T. Supuran, *J. Med. Chem.* **2012**, *55*, 9619.
[25] S. Salerno, E. Barresi, G. Amendola, E. Berrino, C. Milite, A. M. Marini, F. Da Settimo, E. Novellino, C. T. Supuran, S. Cosconati, S. Taliani, *J. Med. Chem.* **2018**, *61*, 5765.
[26] G. J. Kumar, H. V. S. Sriramkumar Bomma, E. Srihari, S. Shrivastava, V. G. M. Naidu, K. Srinivas, V. Jayathirtha Rao, *Med. Chem. Res.* **2013**, *22*, 5973.
[27] G. J. Kumar, S. N. Kumar, D. Thummuri, L. B. S. Adari, V. G. M. Naidu, K. Srinivas, V. J. Rao, *Med. Chem. Res.* **2015**, *24*, 3991.
[28] S. Cascioferro, B. Parrino, V. Spanò, A. Carbone, A. Montalbano, P. Barraja, P. Diana, G. Cirrincione, *Eur. J. Med. Chem.* **2017**, *142*, 523.
[29] D. Maliszewski, D. Drozdowska, *Pharmaceuticals* **2022**, *15*, 221.
[30] L. Guntuku, J. K. Gangasani, D. Thummuri, R. M. Borkar, B. Manavathi, S. Ragampeta, J. R. Vaidya, R. Sistla, N. G. M. Vegi, *Oncogene* **2018**, *38*, 581.
[31] A. S. Negi, Y. Gautam, S. Alam, D. Chanda, S. Luqman, J. Sarkar, F. Khan, R. Konwar, *Bioorg. Med. Chem.* **2015**, *23*, 373.
[32] L. Li, S. Jiang, X. Li, Y. Liu, J. Su, J. Chen, *Eur. J. Med. Chem.* **2018**, *151*, 482.
[33] K. Balmanno, S. J. Cook, *Cell Death Differ.* **2009**, *16*, 368.
[34] I. Marzo, J. Naval, *Biochem. Pharmacol.* **2013**, *86*, 703.
[35] V. Čermák, V. Dostál, M. Jelínek, L. Libusová, J. Kovář, D. Rösel, J. Brábek, *Eur. J. Cell Biol.* **2020**, *99*, 151075.
[36] J. J. Vicente, L. Wordeman, *Exp. Cell Res.* **2015**, *334*, 61.
[37] E. Nogales, *Annu. Rev. Biochem.* **2000**, *69*, 277.
[38] B. Gigant, A. Cormier, A. Dorléans, R. B. G. Ravelli, M. Knossow, *Top. Curr. Chem.* **2008**, *286*, 259.
[39] P. B. Schiff, J. Fant, S. B. Horwitz, *Nature* **1979**, *277*, 665.
[40] M. A. Jordan, L. Wilson, *Nat. Rev. Cancer* **2004**, *4*, 253.
[41] C. F. Beyer, N. Zhang, R. Hernandez, D. Vitale, T. Nguyen, S. Ayral-Kaloustian, J. J. Gibbons, *Cancer Chemother. Pharmacol.* **2009**, *64*, 681.
[42] A. V. Dolzhenko, W. K. Chui, A. V. Dolzhenko, *J. Heterocycl. Chem.* **2006**, *43*, 1513.
[43] G. Gulyás, T. Emri, A. Simon, Z. Györgydeák, *Folia. Microbiol.* **2002**, *47*, 29.
[44] G. Bocci, A. Di Paolo, R. Danesi, *Angiogenesis* **2013**, *16*, 481.
[45] L. Mavroeidis, H. Sheldon, E. Briasoulis, M. Marselos, P. Pappas, A. L. Harris, *Int. J. Oncol.* **2015**, *47*, 455.
[46] G. Bocci, A. Fioravanti, P. Orlandi, T. di Desidero, G. Natale, G. Fanelli, P. Viacava, A. G. Naccarato, G. Francia, R. Danesi, *Neoplasia* **2012**, *14*, 833.
[47] F. Vaglini, C. Pardini, T. Di Desidero, P. Orlandi, F. Pasqualetti, A. Ottani, S. Pacini, D. Giuliani, S. Guarini, G. Bocci, *Mol. Neurobiol.* **2018**, *55*, 4984.

SUPPORTING INFORMATION

Additional supporting information can be found online in the Supporting Information section at the end of this article.

How to cite this article: M. Robello, S. Salerno, E. Barresi, P. Orlandi, F. Vaglini, M. Banchi, F. Simorini, E. Baglini, V. Poggetti, S. Taliani, F. Da Settimo, G. Bocci, *Arch Pharm*. **2022**, e2200295. https://doi.org/10.1002/ardp.202200295